P-S survey design

Liliana M. Zuleta and Don C. Lawton

ABSTRACT

Fold, illumination, offset distribution and azimuth distribution were evaluated for PS survey design for two different projects. The first was planned to image an interval of interest from 380 m to 425 m depth, for the Paskapoo Formation, located in the Priddis area. Orthogonal and slant geometries were tested with different parameters. Good results for the converted wave 3D design were found using a slant geometry design with receiver interval and source interval of 10 m, a receiver line interval of 50 m, a source line interval of 25 m and a maximum offset of 400 m. Fold for the slant geometry design gave better offset and azimuth distributions than the orthogonal geometry design. Illumination was similar in both types of geometries. Optimization of these parameters was reached by changing the receiver and source line intervals to 40 m, balancing quality requirements and cost related to the increase of number of shots when using 25 m as the source line interval. This design was done using CREWES QuadDes software.

A second case study was undertaken where orthogonal and slant designs were also both tested for a project area with a deeper target, at 2160 m depth, and a shallow horizon of interest at 500 m. Real situations were taken in to consideration such as having to move source lines to pre-existing cut lines and examing the effect of obstructions presented by lakes in the area of the survey. After the analysis, an orthogonal geometry design was chosen with 360 m source line interval, 240 m receiver line interval and 60 m source and receiver station intervals. The patch selected was 26 lines with 100 receivers per line to have an aspect ratio of about unity for optimum data inversion. This design was undertaken using OMNI software.

INTRODUCTION

Fold, illumination, offset distribution and azimuth distribution were evaluated for PS survey design for two different projects.

The main objective of the first project (shallow target) was to design a P-S survey with optimum parameters in a way that seismic attributes such as fold, offset distribution and azimuth distribution are as good values as those offered by a P-P survey design. Different programs were used: Syngram to generate the synthetic seismogram needed to find the maximum offset and QuadDes to make the design with different parameters and generate plots of seismic attributes.

The main objective of the second project (deep target), was to analyze the geometry footprint of acquisition. Acquisition footprint refers to patterns seen on 3D seismic time slices that reflect the geometry used to acquire the survey or some features present on the surface like rivers, lakes or any other obstruction. For this study OMNI software was used.

Shallow target design – Paskapoo Formation

The P-S 3D seismic survey design was performed to illuminate the prospective interval shown in Figure 1 (red lines indicate top and bottom of the interval of interest). The depth of this interval is from 380 m to 425 m and corresponds to the Paskapoo Formation. This formation occurs east of the Canadian Rockies in the foothills; it was deposited in a fluvial and deltaic depositional environment reaching a maximum depth of 600 m.

The Paskapoo Formation of southern Alberta is an extensive Paleocene-aged fluvial mudstone and sandstone complex covering ~65000 km^2 or ~10% of Alberta. It ranges from 0 to 800 m thickness and represents the youngest bedrock deposits in the Western Canada Sedimentary Basin (WCSB). It comprises greenish sandy siltstone and mudstone, with light grey, thick-bedded sandstone, deposited in non marine environments. In the Plains, the strata are near horizontal, dipping westward at <1° as a homoclinal wedge into the core of the Alberta syncline. The unit is >50% siltstone and mudstone (Grasby, 2008).

Maximum Offset determination

QuadDes Software was used to make a PS survey design which offers two methods for this type of design: P-S asymptotic and P-S depth-specific. The latter was used for this project because is the recommended approach for P-S surveys. This algorithm maps the true depth-variant position of conversion points for the same source-receiver offset. The depth specific conversion point (DSCP) binning uses a ray tracing scheme via input of a depth, z, to a specific target reflector and a Vp/Vs over this depth interval. The value for Vp/Vs used was 2.2 due to the high values of Gamma ray log (see figure 1), from which shaly formation was inferred.

Sonic and density logs were provided for well 12-33 shown in Figure 1. Vp was determined from the sonic log. With Vp/Vs=2.2, Vs was calculated from Vp using Syngram to generate the synthetic seismogram. The maximum offset to be used efficiently can be determined from this synthetic seismogram (Figure 2) beyond which traces become affected by stretch and phase rotation; this occurs around 300 m to 400 m.

Survey Design Parameters

The followings are the parameters used to carry out the design for two geometries: orthogonal and slant with an angle of 45 degrees (Figure 3).

Fold: 50

Survey Area: 600 x 600 m

Interval of interest: 380 m – 425 m

Vp/Vs: 2.2

For this part of the project, receiver interval, receiver line interval and source interval were kept fixed; source line interval and maximum offset were changed to see how the design is affected and then to choose the best option. Subsequently, a comparison with P-P survey design, the effect of changing receiver line interval and the results of changing Vp/Vs ratio are presented. A summary of the parameters used are shown in Table 1.

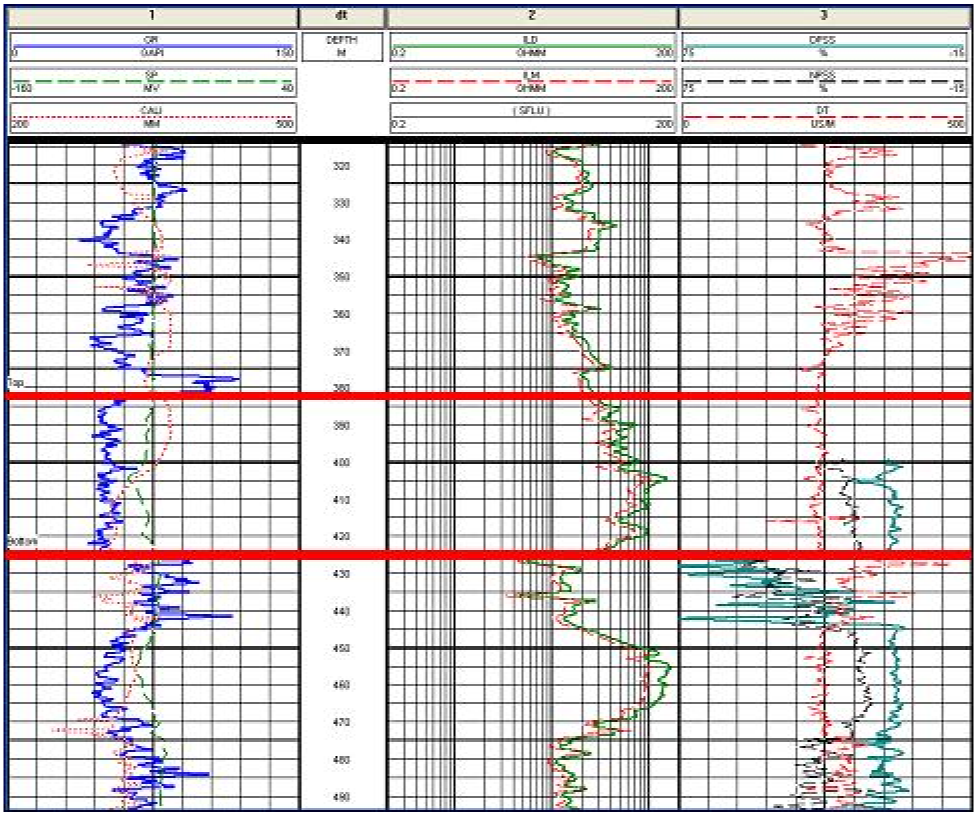

FIG. 1 Well RENAISSANCE ET AL MILLAR 12-33-21-2, field : MILLARVILLE

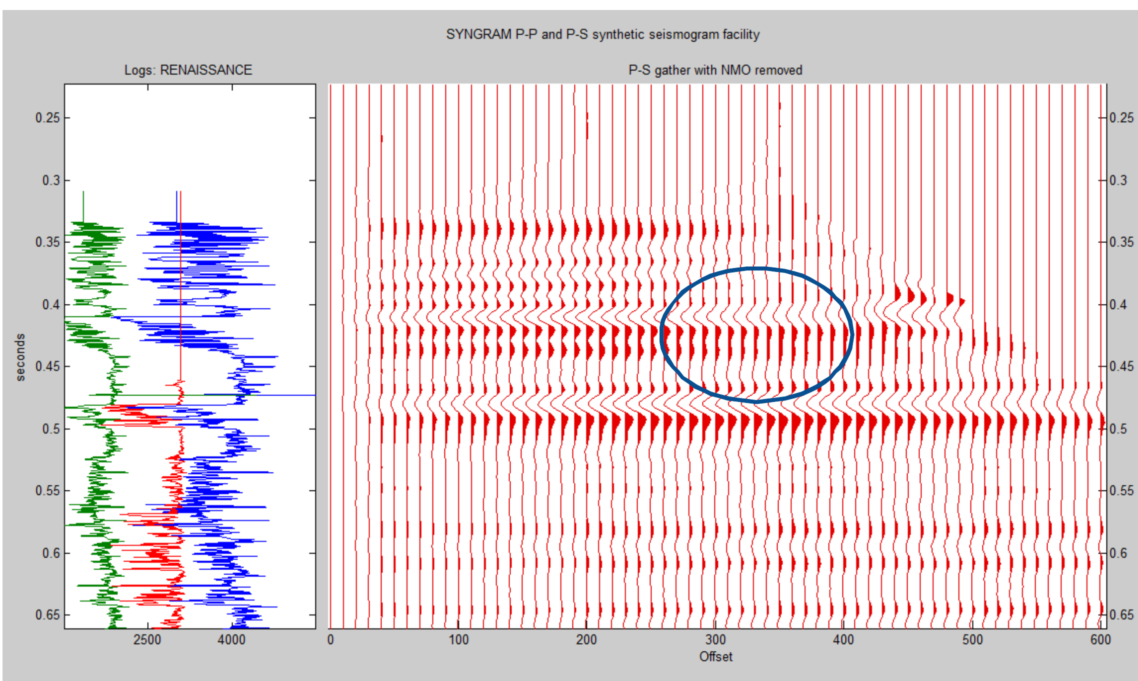

FIG 2. Synthetic seismogram generated from Syngram

Table 1. Survey design parameters

	Model 1	Model 2	Model 3	Model 4
Geometry	Orthogonal	Orthogonal	Slant-45	Slant-45
Receiver Interval	10 m	10 m	10 m	10 m
Receiver line Interval	50 m	50 m	50 m	50 m
Source Interval	10 m	10 m	10 m	10 m
Source line Interval	50 m	25 m	50 m	25 m
Max Offset	300-400 m	300-400 m	300-400 m	300-400 m

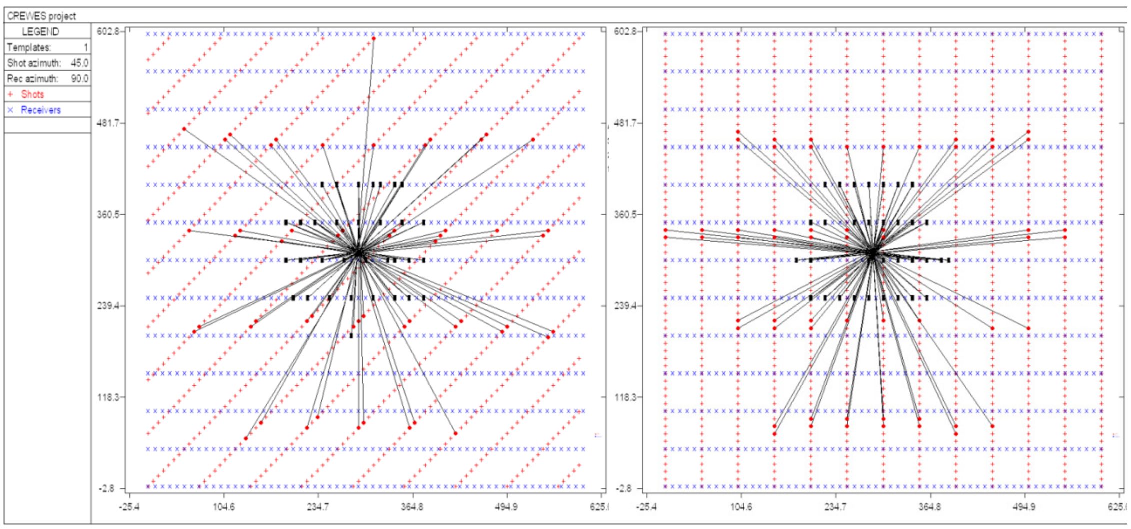

FIG. 3. Slant Geometry (left) and Orthogonal Geometry (right) with example ray path projection

Results

A set of attribute results are presented, using the design parameters shown in Table 1. Figure 4 shows the fold for the orthogonal survey geometry with source line interval of 50 m (top) and 25 m (bottom), and maximum offsets of 300 m (right) and 400 m (left). This figure shows how this kind of geometry produces an irregular fold distribution that is improved using the slant geometry, presented in Figure 5.

For P-S survey, it is better to evaluate illumination which is a fold interpolation. Illumination is essentially fold mapped to neighbouring bins in the case when reflection points are not bin-centred (from QuadDes help manual). Figures 6 and 7 show the results of illumination for the orthogonal and slant geometry, respectively. It is noticeable that the coverage is more continuous and now there is less difference between both geometry results (orthogonal and slant). Fold increases when the maximum offset is larger and increases more when the source line interval is smaller. The coverage is almost double when extending the maximum offset from 300 m to 400 m and also when decreasing the source line interval from 50 m to 25 m.

The minimum fold required for this design was 50. Both geometries reached this value in almost 80 % of the area when offset is 400 m and source line interval is 25 m.

Figures 8 and 9 show the offset distribution quality for orthogonal and slant geometries, respectively. The quality factor lies between values of 0 and 1. A value of 1 means that at least one trace representing each offset panel is presented in the bin (good quality). The results for orthogonal geometry shows footprint of the surface lay out that is not present with slant geometry. Offset distribution quality increases when the maximum offset increases and the source line interval decreases for both orthogonal and slant geometries.

Figures 10 and 11 show the azimuth distribution quality for orthogonal and slant geometries, respectively. The quality factor lies between values of 0 and 1. If all azimuth sectors contain at least one trace, it produces a value of 1. The results for orthogonal geometry show irregularities in azimuth distribution that are smoother in slant geometry. Azimuth distribution quality also increases when maximum offset increases and source line interval decreases. From the set of parameters tested, the best results are obtained using a slant geometry with 25 m source line interval and a maximum offset of 400 m.

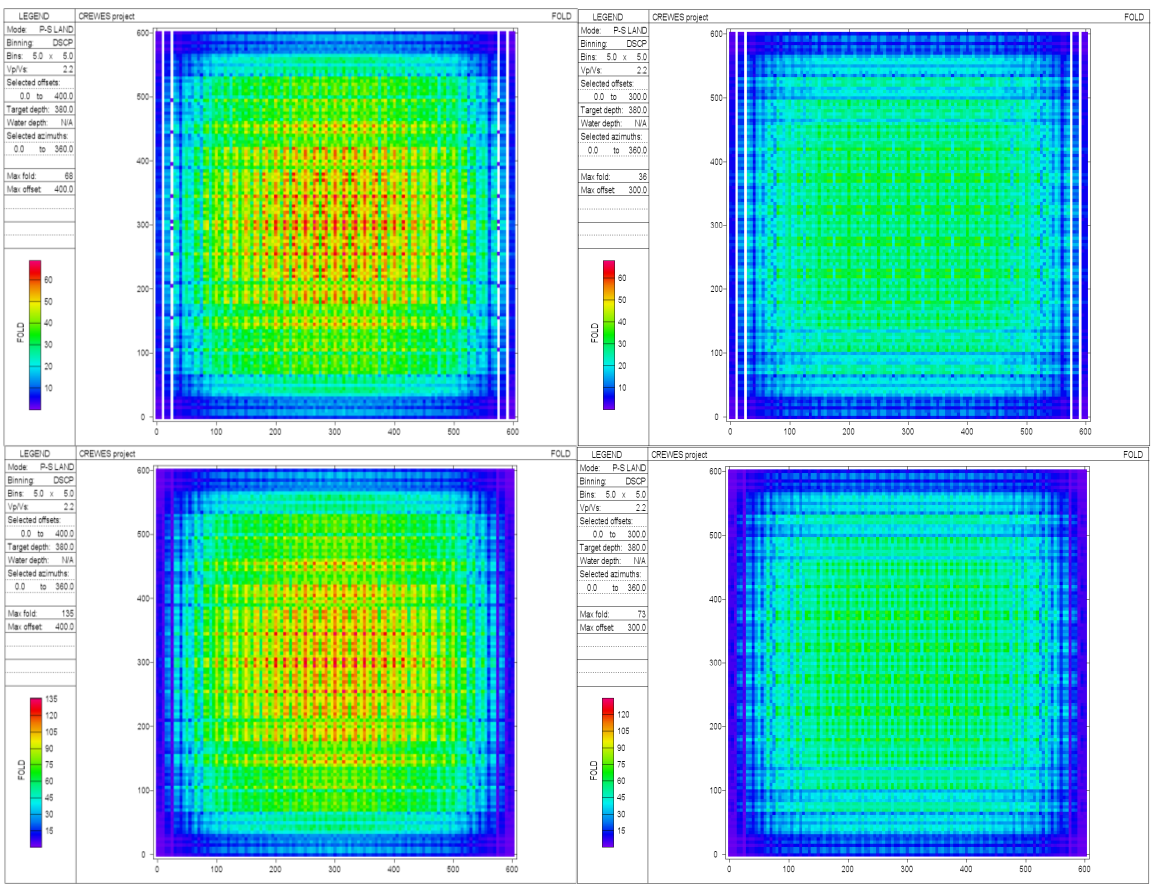

FIG 4. Fold – Orthogonal Geometry. Top Left: Model 1–Max offset= 400 m, Top right: Model 1–Max offset= 300 m, bottom left: Model 2–Max offset= 400 m; bottom right: Model 2–Max offset= 300 m. (Models 1 to 4 according to table 1)

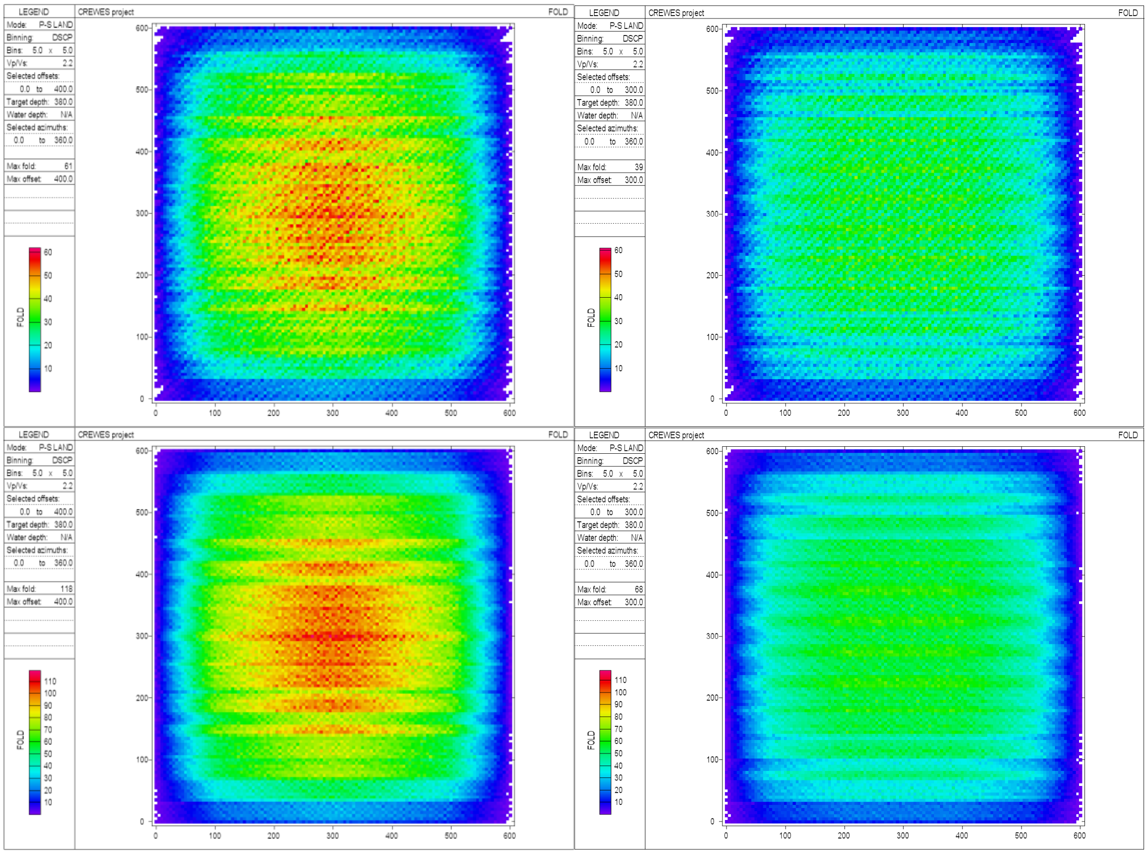

FIG. 5. Fold – Slant Geometry. Top Left: Model 3 – Max offset=400 m, Top right: Model 3–Max offset=300 m, bottom left: Model 4 – Max offset=400 m; bottom right: Model 4–Max offset=300 m. (Models 1 to 4 according to table 1)

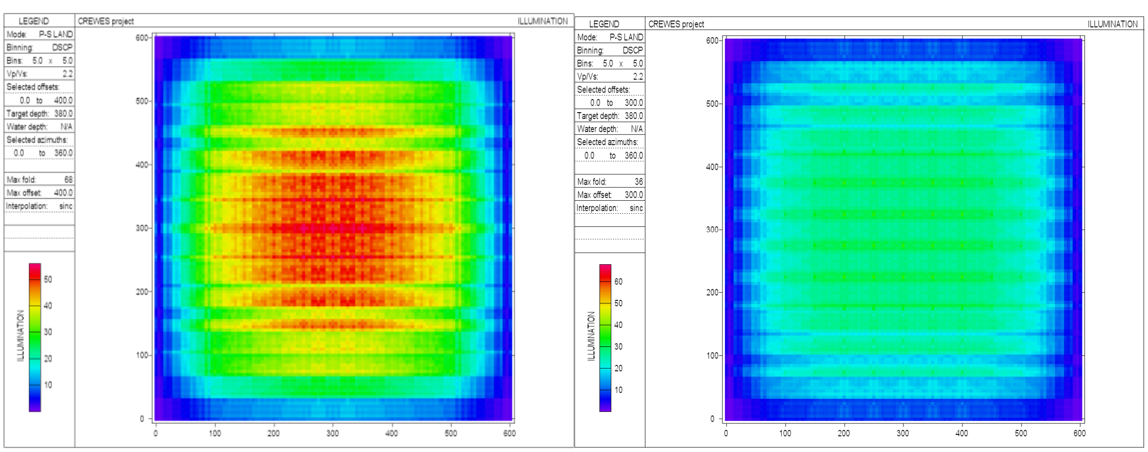

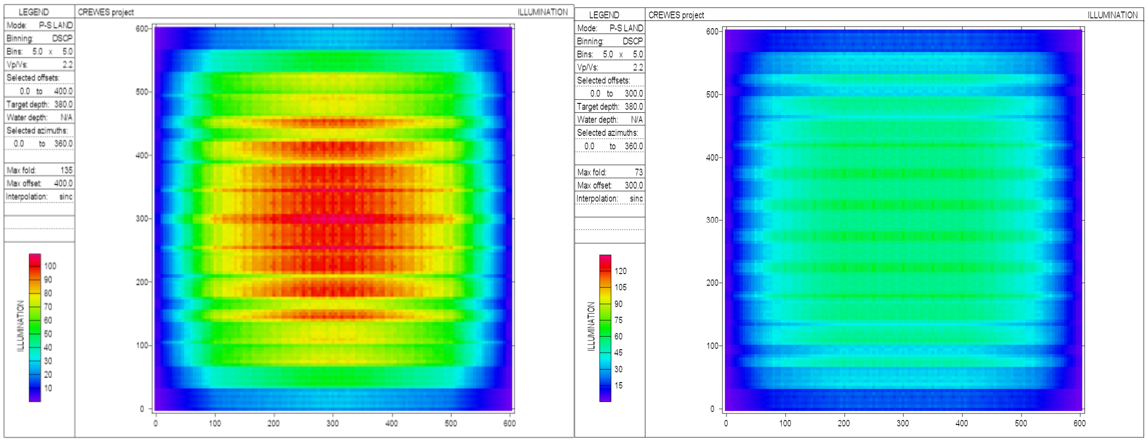

FIG. 6. Illumination – Orthogonal Geometry. Top Left: Model 1 – Max offset=400 m, Top right: Model 1 – Max offset=300 m, bottom left: Model 2 – Max offset=400 m; bottom right: Model 2 – Max offset=300 m. (Models 1 to 4 according to table 1)

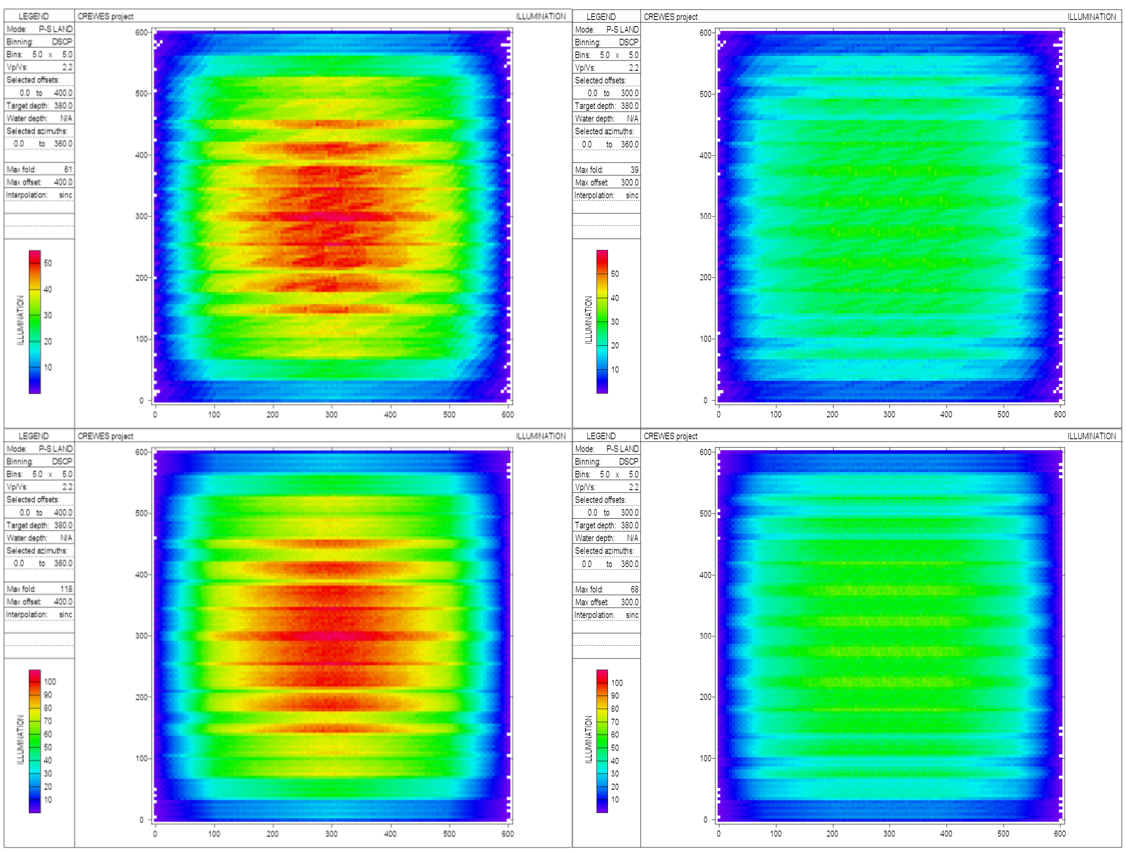

FIG. 7. Illumination – Slant Geometry. Top Left: Model 3 – Max offset=400 m, top right: Model 3 – Max offset=300 m, bottom left: Model 4 – Max offset=400 m; bottom right: Model 4 – Max offset=300 m. (Models 1 to 4 according to table 1)

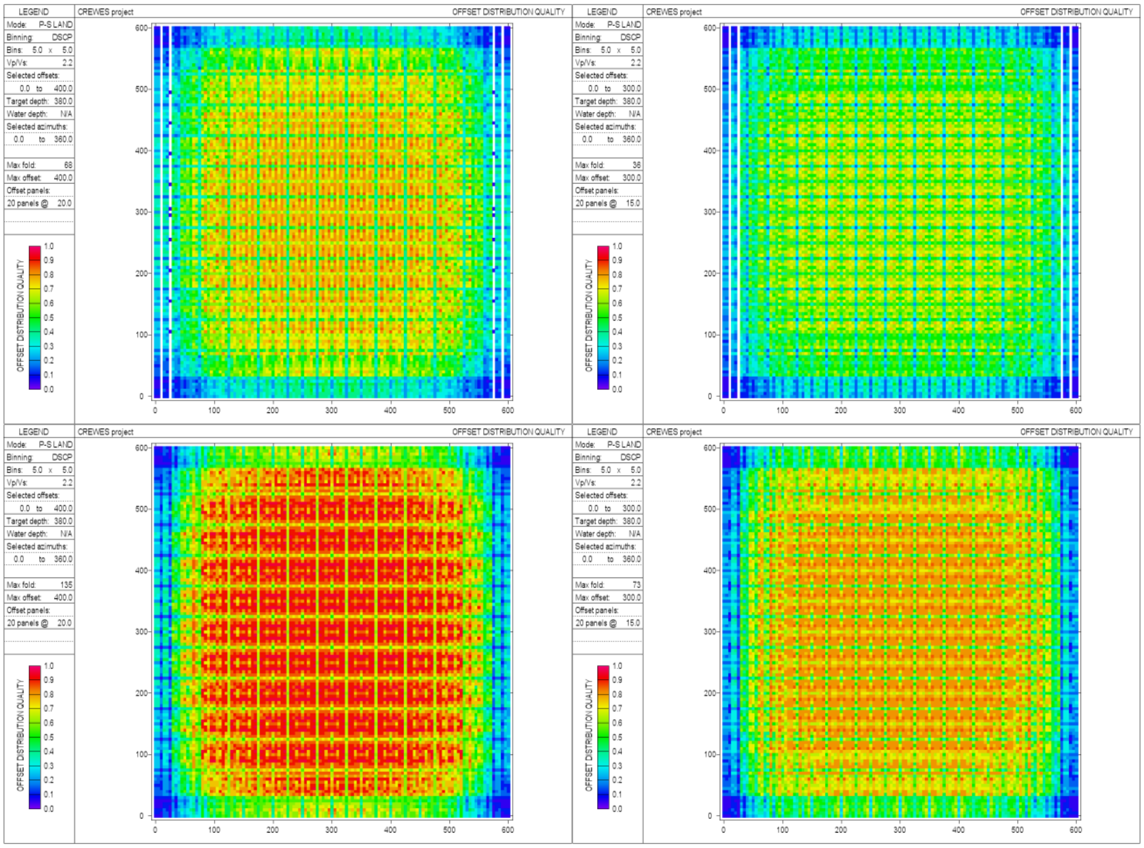

FIG. 8. Offset distribution quality – Orthogonal Geometry. Top Left: Model 1 – Max offset=400 m, top right: Model 1 – Max offset=300 m, bottom left: Model 2 – Max offset=400 m; bottom right: Model 2 – Max offset=300 m. (Models 1 to 4 according to table 1)

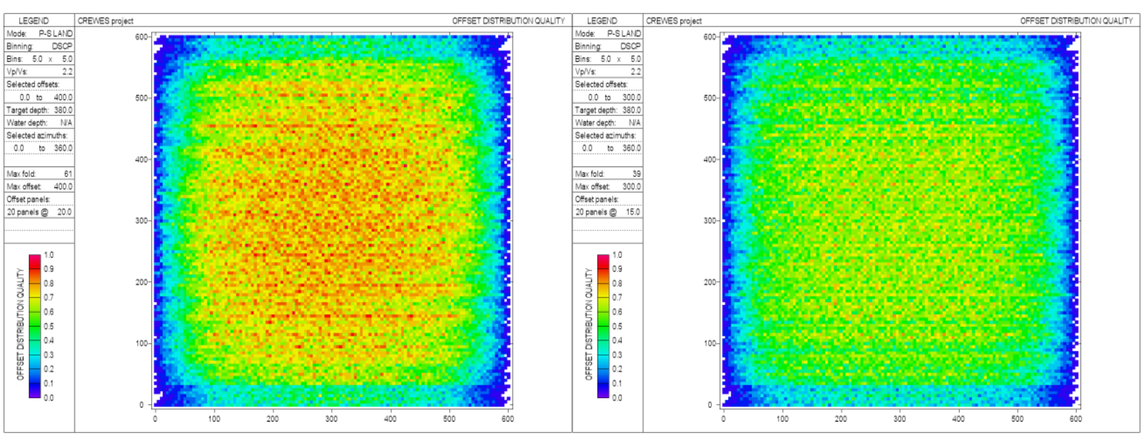

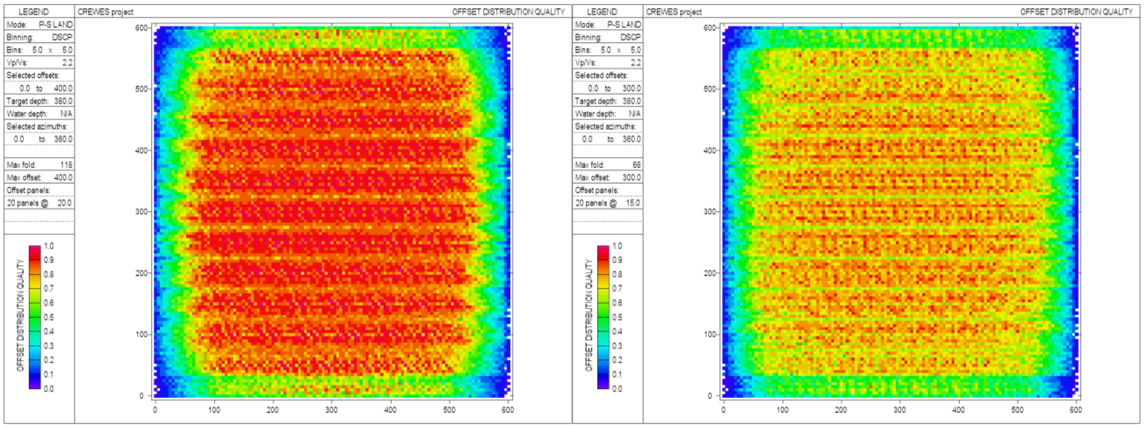

FIG. 9. Offset distribution quality – Slant Geometry. Top Left: Model 3 – Max offset=400 m, top right: Model 3 – Max offset=300 m, bottom left: Model 4 – Max offset=400 m; bottom right: Model 4 – Max offset=300 m. (Models 1 to 4 according to table 1)

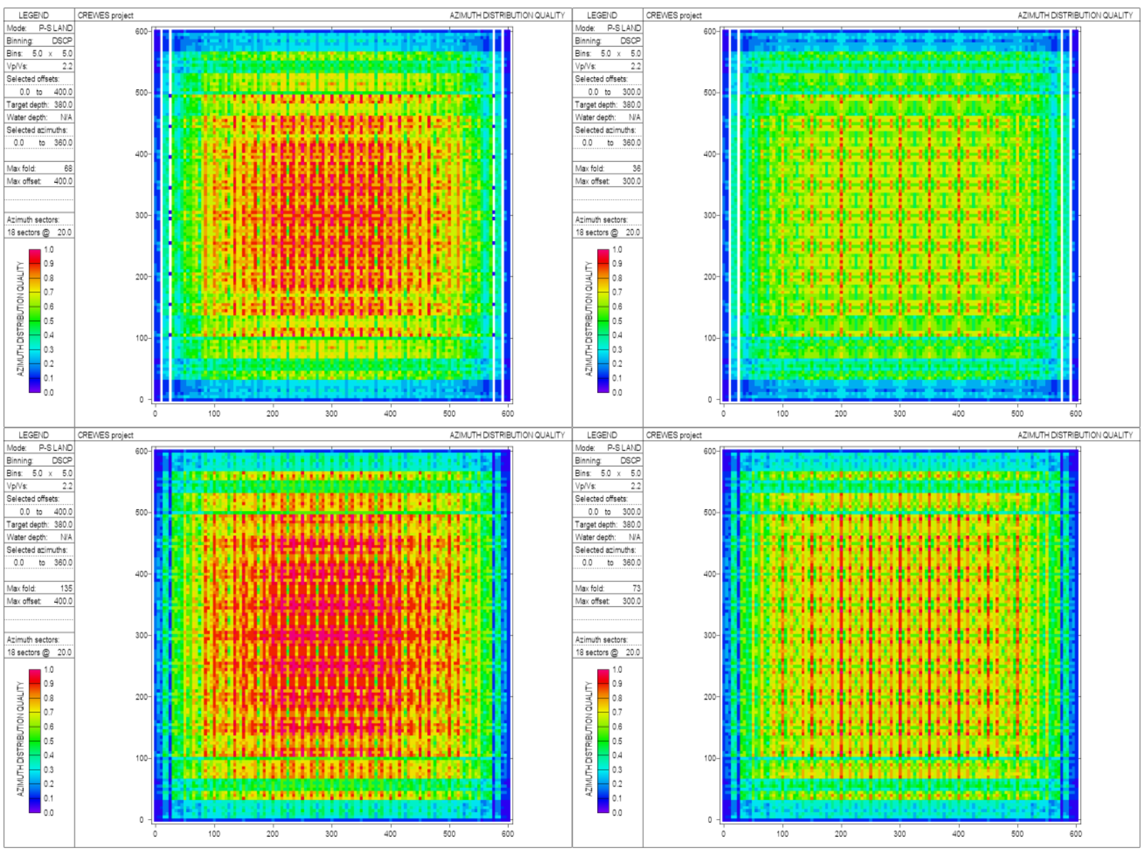

FIG. 10. Azimuth distribution quality – Orthogonal Geometry. Top Left: Model 1 – Max offset=400 m, top right: Model 1 – Max offset=300 m, bottom left: Model 2 – Max offset=400 m; bottom right: Model 2 – Max offset=300 m. (Models 1 to 4 according to table 1)

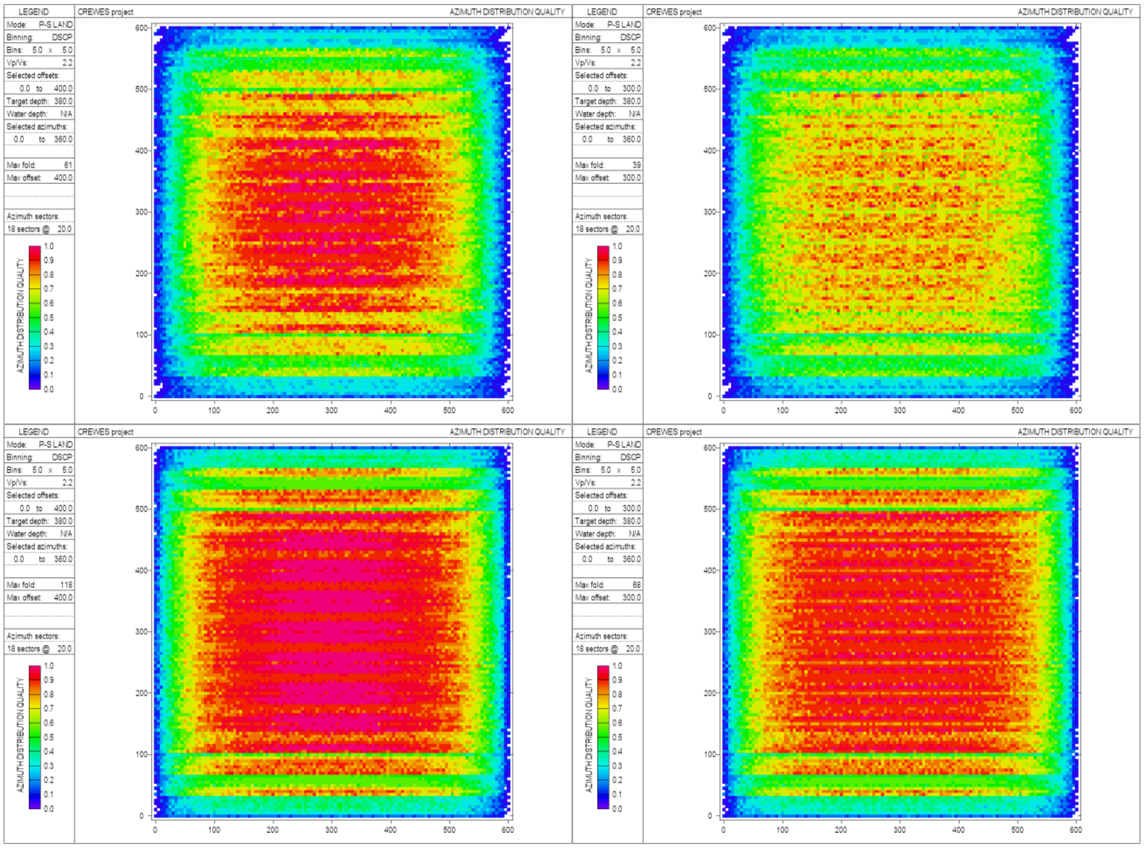

FIG. 11. Azimuth distribution quality – Slant Geometry. Top Left: Model 3 – Max offset=400 m, top right: Model 3 – Max offset=300 m, bottom left: Model 4 – Max offset=400 m; bottom right: Model 4 – Max offset=300 m. (Models 1 to 4 according to table 1)

Discussion

After defining what is likely to be the optimum design parameters, some additional comparison are needed. The optimum parameters were used to make three tests: first a comparison of results with a P-P survey design, then decreasing receiver line interval to try to improve fold distribution and finally two different values of Vp/Vs were used to identify the effect on the seismic attributes.

Figure 12 shows fold (top), offset distribution quality (bottom left) and azimuth distribution quality (bottom right) for a P-P survey design for orthogonal geometry. This image was compared with the result for P-S survey design shown in the lower left of Figure 6 (illumination), Figure 8 (offset) and Figure 10 (azimuth). It is observed that the requirement of 50 fold is accomplished but a horizontal pattern of low and high values of fold is noticed in the P-S design. Remember that continuous fold is required to have robust post-stack amplitude mapping as well as pre-stack amplitude versus offset (AVO) analysis, particularly for evaluating azimuthal dependence (Lawton, 1993).

The offset distribution diagram shows that the footprint effect of the surface lay out and the azimuth diagram shows irregularities in the P-S results compared to P-P results.

Figure 13 shows fold (top), offset distribution quality (bottom left) and azimuth distribution quality (bottom right) for a P-P survey design for slant geometry. This image was compared with the result for P-S survey design shown in the lower left of Figure 7 (illumination), Figure 9 (offset) and Figure 11 (azimuth). The fold, as in the orthogonal case, reached the required 50 fold but with the same horizontal pattern of low and high values of fold. The offset and azimuth distribution show better response for slant geometry than for the orthogonal geometry, being closer to the P-P survey design. This result confirms this type of geometry as being superior to orthogonal design.

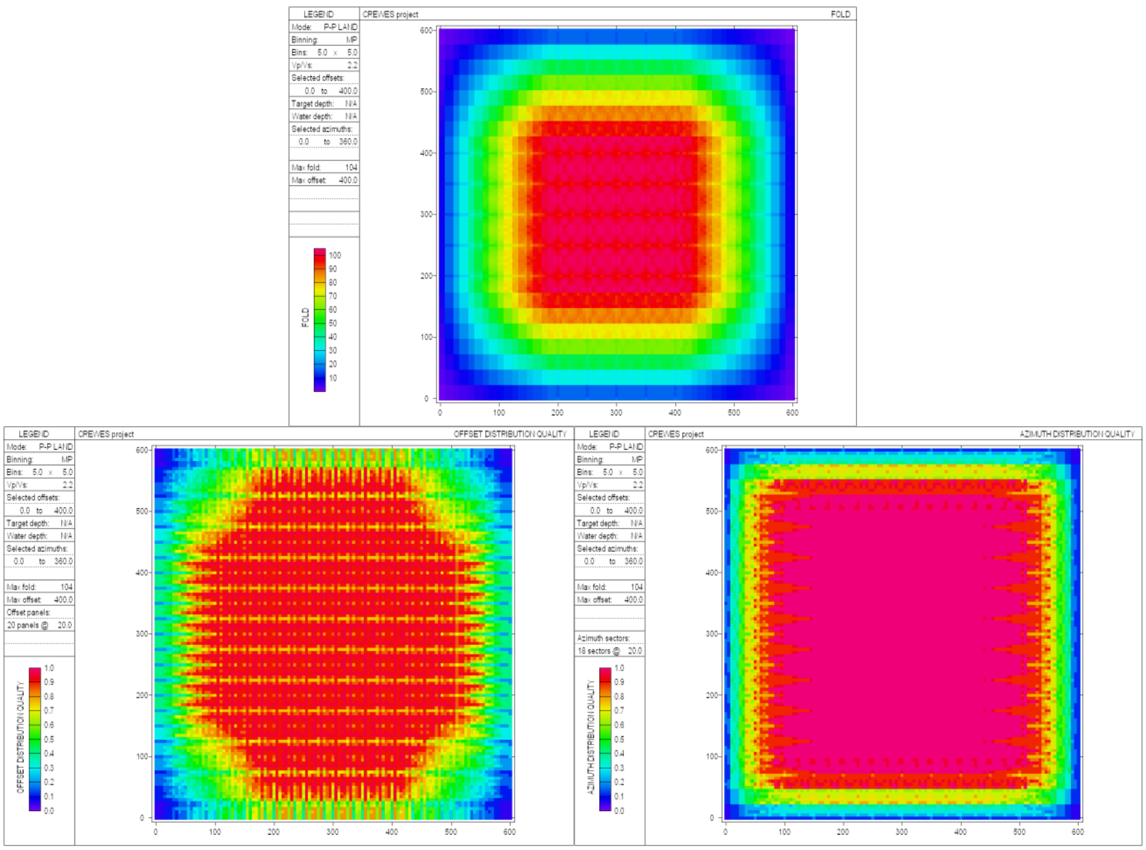

FIG. 12. P-P Survey design – Orthogonal Geometry. Fold (top), Offset distribution quality (bottom left) and Azimuth distribution quality (bottom right)

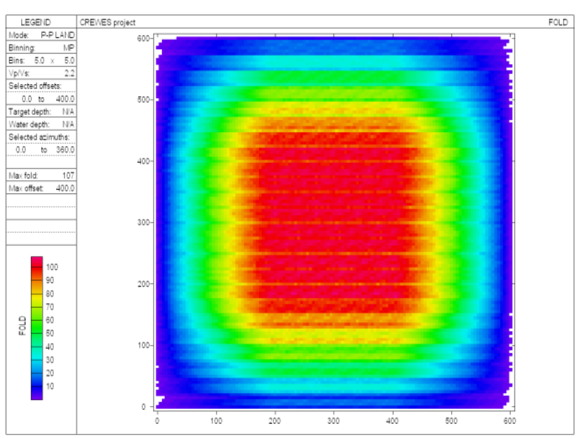

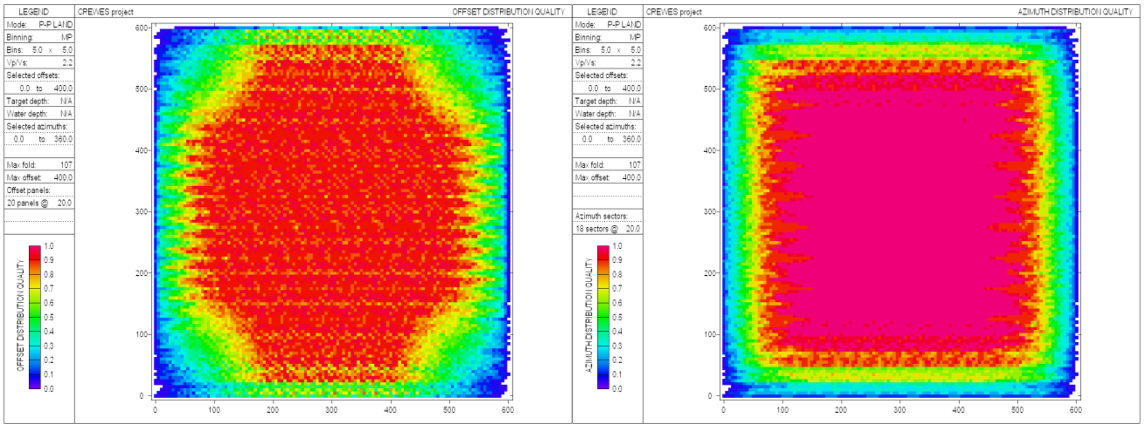

FIG. 13. P-P Survey design – Slant Geometry. Fold (top), Offset distribution quality (bottom left) and Azimuth distribution quality (bottom right)

The bin size for converted wave 3D could be larger that bins for the compressional wave (Lawton, 1993), therefore the fold would be higher for converted wave than for compressional wave bins (Cordsen and Lawton, 1996).

Figure 14 shows the ray path differences between P-S and P-P reflections (plan view). In converted waves, the reflection point is not centered between source and receiver points. The conversion point lies closer to the receiver points, depending on the Vp/Vs ratio (Figure 15). At higher ratios, the conversion points get closer to the receiver.

The horizontal pattern of low and high fold mentioned earlier can be improved by decreasing the receiver line interval. The receiver line interval was decreased to 40 m. The results are shown in Figure 16 for orthogonal geometry and Figure 17 for slant geometry.

Fold distribution improves using 40 m receiver line interval compared with the result of 50 m receiver line interval, the pattern is smoother and is closer to the P-P fold distribution. As expected, the value of fold increases obtaining a value much higher than the required 50 fold but also the area covered with this value is greater. Offset and azimuth distribution do not change the initial pattern: footprint of surface lay out in orthogonal geometry is presented and better distribution with slant geometry.

Figure 18 shows the effect of the changes of Vp/Vs ratio over illumination (fold). It can be noticed that at higher values of Vp/Vs ratio, the horizontal pattern of low and high fold gets stronger (higher contrast of fold). This result can be related with the definition of converted point separation (from Crewes Sponsor lecture):

$Xc = r/(1+Vs/Vp)$ Inline separation

$Xc = s/(1+Vp/Vs)$ Xline separation

Where r is the receiver interval and s is the source interval. If the ratio Vp/Vs is changed in these equations, the variation in conversion point separation will affect more the crossline value that the inline value, which could be the reason why fold irregularities are present as a horizontal pattern dominating in the Xline rather than the inline direction.

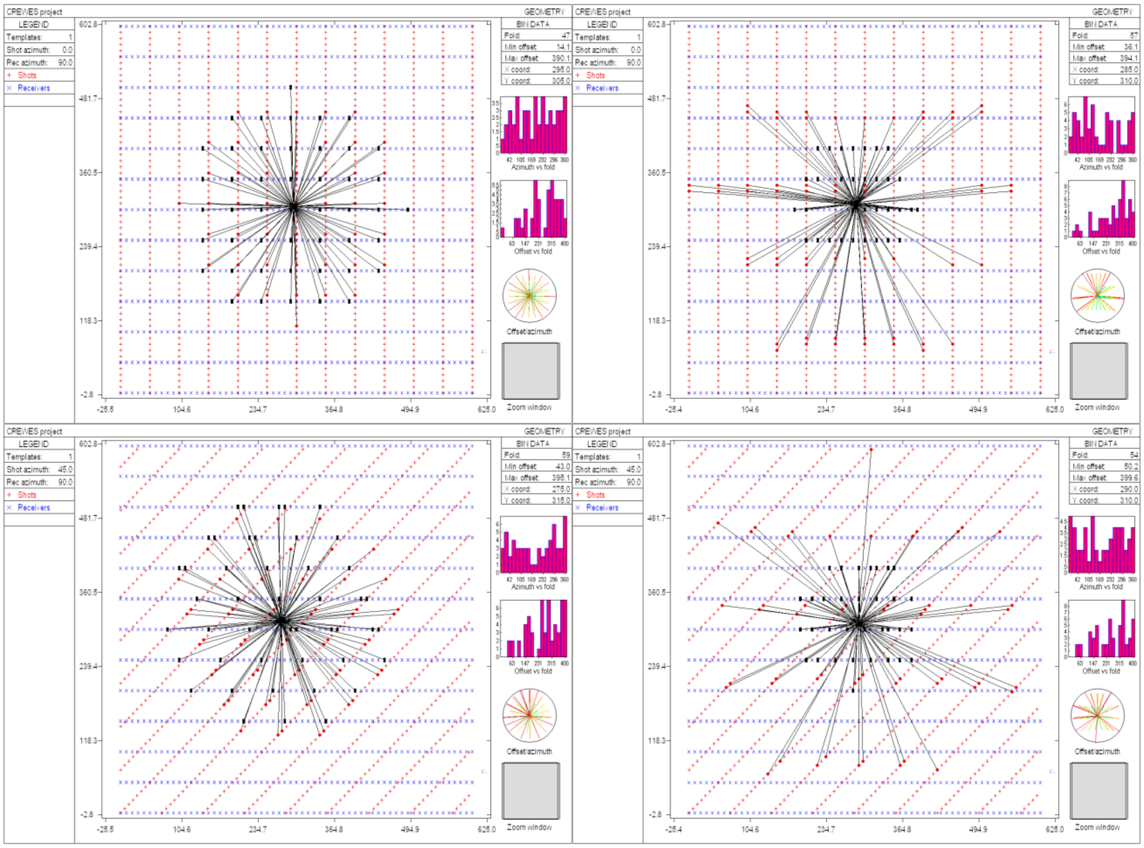

FIG 14 Ray path for P-P and P-S reflections. Top Left: PP Survey – orthogonal, top right: PS Survey – orthogonal, bottom left: PP Survey – Slant; bottom right: PS Survey – Slant

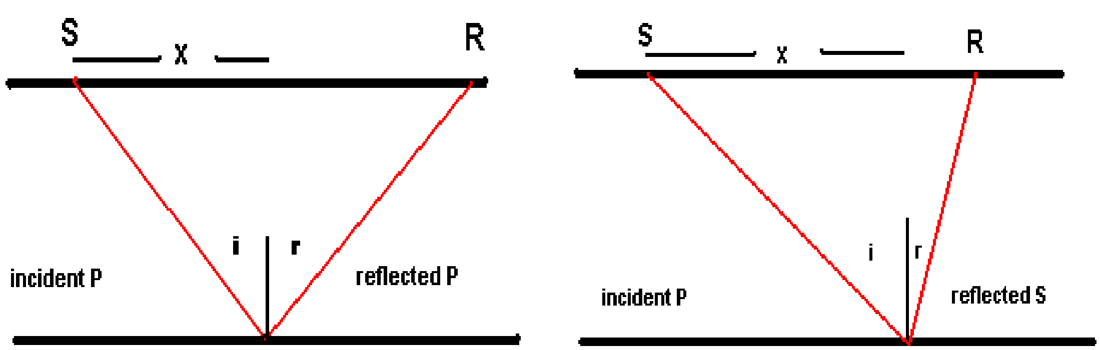

FIG 15. Schematic of common midpoint (left) and Common conversion point (right)

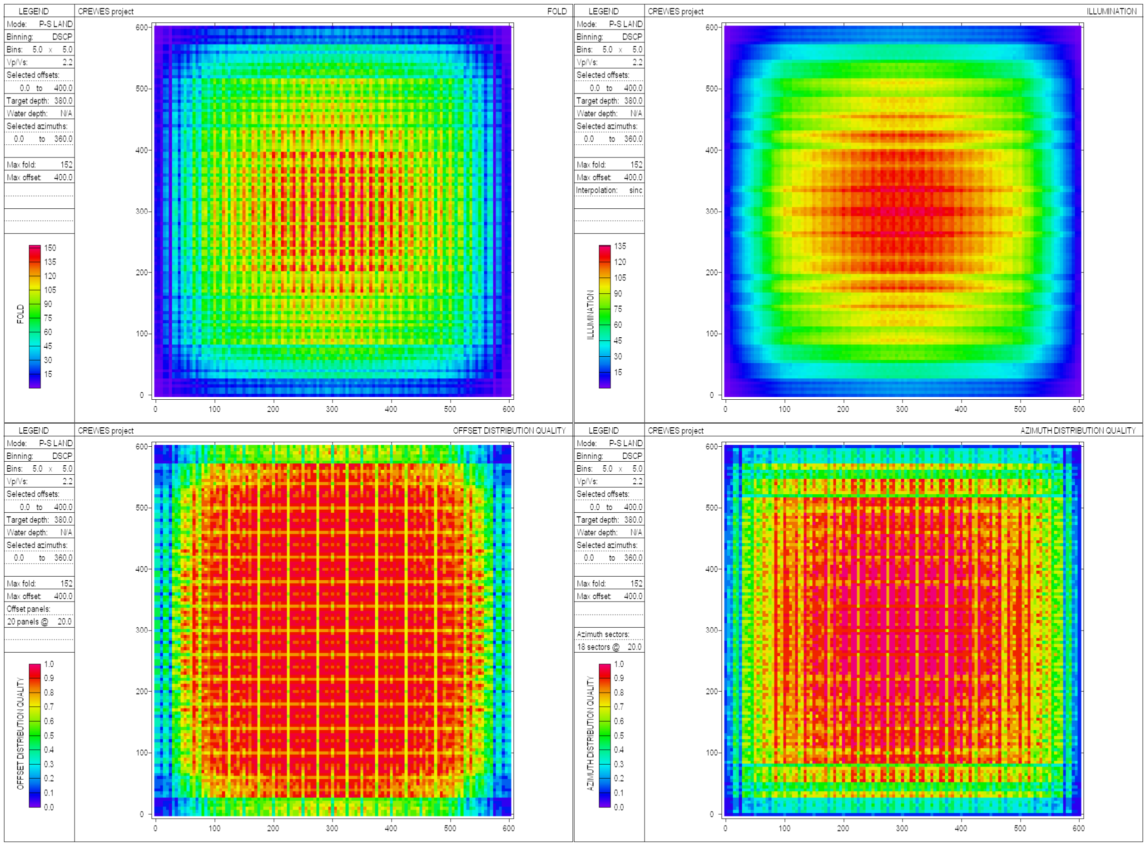

Figure 16 P-S Survey design – Orthogonal – changing receiver line interval to 40 m. Fold (top right), Illumination (top left), Offset distribution quality (bottom left) and Azimuth distribution quality (bottom right)

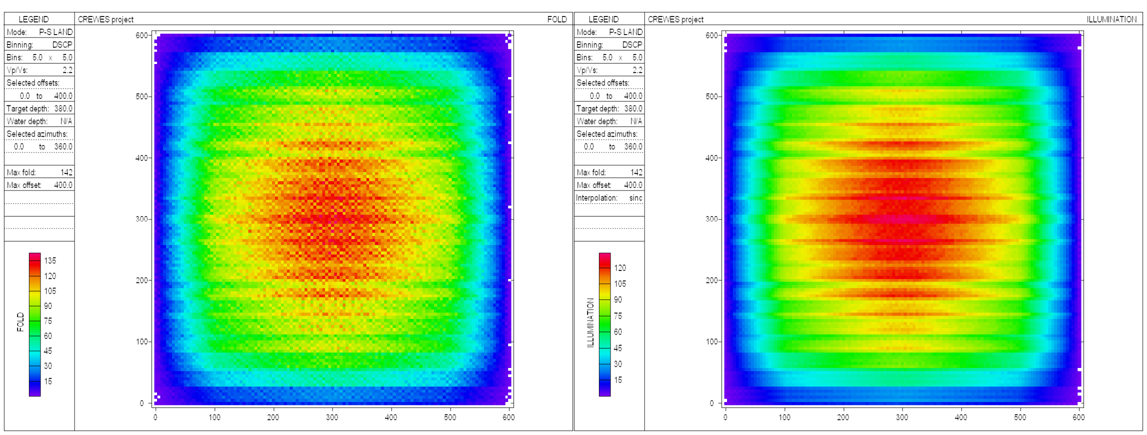

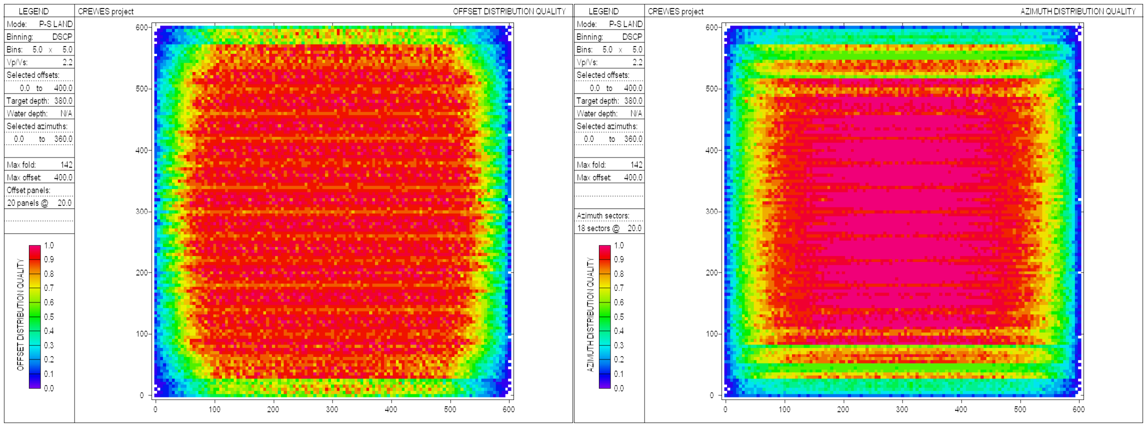

Figure 17 P-S Survey design – Slant - Changing receiver line interval to 40 m. Fold (top right), Illumination (top left), Offset distribution quality (bottom left) and Azimuth distribution quality (bottom right)

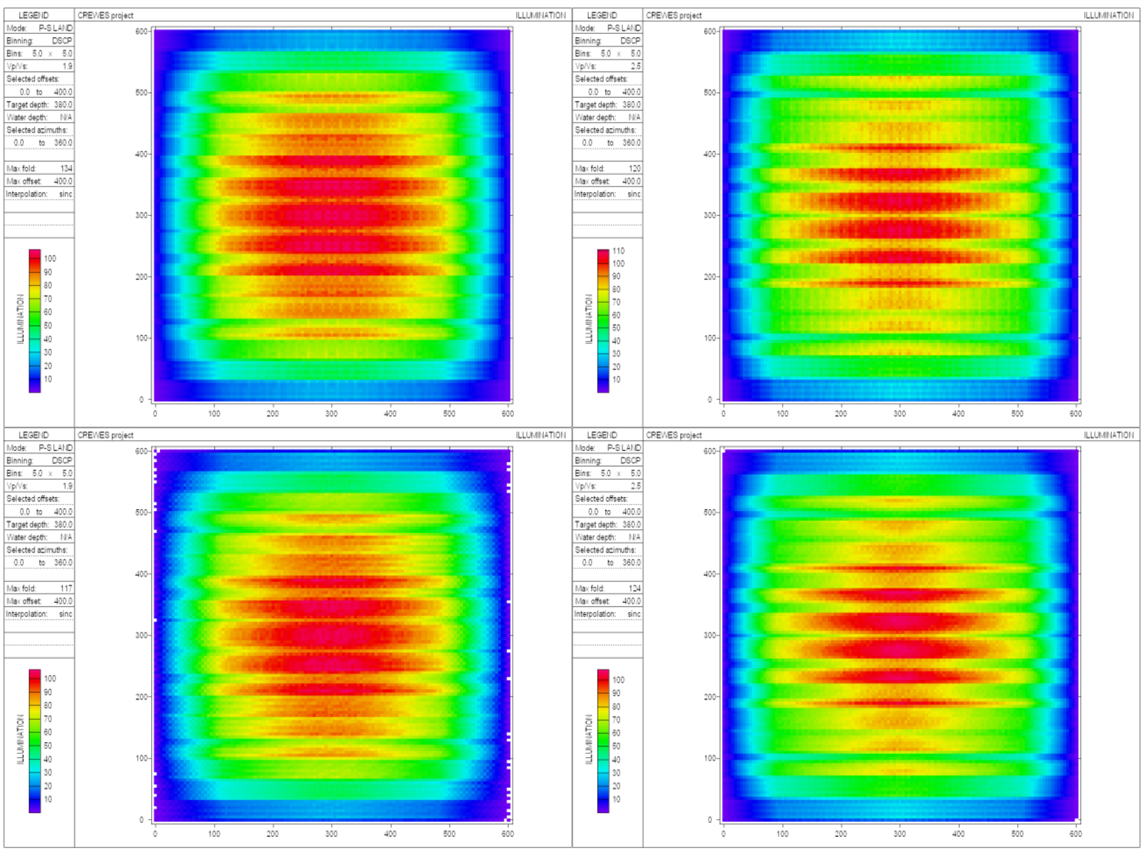

Figure 18 Vp/Vs Variation results over illumination. Top left: Vp/Vs 1.9 – Orthogonal, top right: Vp/Vs 2.5 – Orthogonal, bottom left: Vp/Vs 1.9 – Slant, bottom right: Vp/Vs 2.5 – Slant.

Another important consideration that has to be taken in to account when undertaking survey design is the cost of executing the planned survey. In this example, the best parameters considered is the source line interval of 25 m, source and receiver intervals of 10 m and a receiver line interval of 50 m. Decreasing the source line interval leads to having a higher number of sources, increasing the cost of the acquisition. An alternative to these parameters is to use source and receiver line intervals of 40 m. The results of attributes are shown in Figures 19 and 20 for orthogonal and slant geometries, respectively; the comparison of number of receivers and sources between different design options are shown in Table 2.

It is observed in Table 2 that the number of shots when considering 25 m source line interval is almost double compared to 50 m source line interval. If a 40 m source line interval is considered, the number of shots increases moderately and as shown in Figures 19 and 20, the attributes are comparable with the results of using 25 m. The number of receivers also increases but this factor does not affect in a big magnitude the cost of the acquisition.

Table 2 Statistics for different design options

	Orthogonal			**Slant – 45 degrees**		
DSL	**50 m**	**25 m**	**40 m**	**50 m**	**25 m**	**40 m**
Total Sources	793	1525	976	1020	2040	1275
Total Recs	793		976	793		976

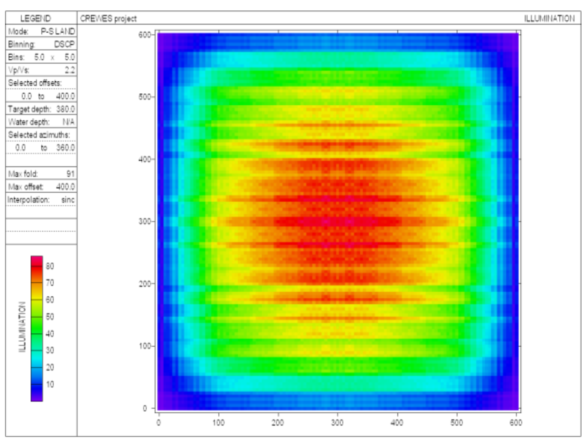

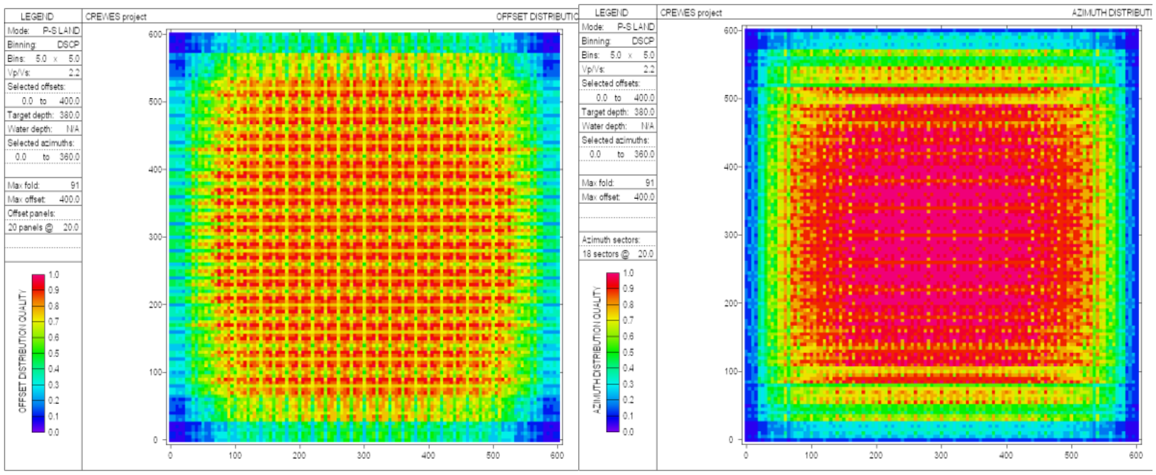

Figure 19 P-S Survey Design – Orthogonal Geometry – 40 m source and receiver line interval. Illumination (top), Offset distribution quality (bottom left) and Azimuth distribution quality (bottom right)

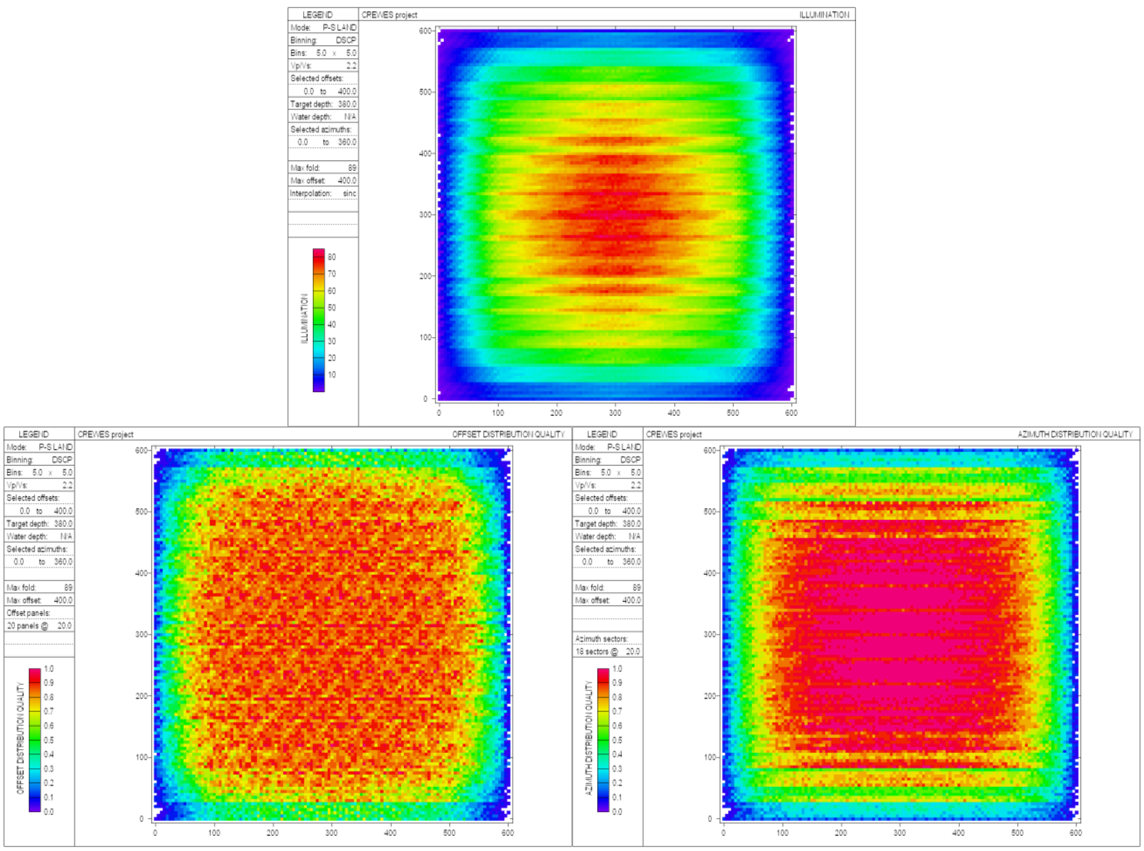

Figure 20 P-S Survey Design – Slant Geometry – 40 m source and receiver line interval. Illumination (top), Offset distribution quality (bottom left) and Azimuth distribution quality (bottom right)

In this case is confirmed again that slant geometry offers better results than orthogonal geometry.

Case Study – Deep Target

The main objective of this case study was to analyze acquisition footprint, which refers to patterns seen on 3D seismic time slices that reflect the geometry used to acquire the survey or some features present on the surface such as rivers, lakes or any other obstruction; these patterns obscure the actual amplitude anomalies under consideration for stratigraphic interpretation, AVO analysis and reservoir attribute studies. For this study OMNI software was used. Four different geometries were tested: Orthogonal, slant, double brick, and triple brick. The last two were discarded due to environmental restrictions (issues of cut lines). The input parameters for the 3D design, obtained from exploration objectives and from existing 2-D seismic data, are shown in Table 3.

Table 3. 3-D design input parameters

Fold of good 2-D data: 96
Steepest dip: 10°
Mute for shallow markers needed for isochroning: 500 m (shallow target)
Target depth: ~2700 m
Target two way time: 2.9 s
V_{int} immediately above the target horizon: 2880 m/s – 3440 m/s
F_{dom} at the target horizon: ~50 hz
F_{max} at the target horizon: ~80 hz
Lateral target size: N/A
Area to be fully imaged: 300 km^2
Layout method: Orthogonal and Slant

Based on this information the initial survey design parameters were calculated. The results are shown in Table 4.

Table 4. 3-D design flowchart

Desired fold= 48	(1/2 to 1) full 2D fold = 48 -96
Bin Size (B)	a) For target size: B= N/A b) For alias frequency: $B_1= V_{int} / (4*f_{max} * \sin\theta)$ If V_{int}= 2880, B_2= <u>51.8 m</u>; If V_{int}= 3440, B_2= <u>61.9 m</u> c) For lateral resolution: $B_1= V_{int}/(N*f_{dom})$ =28.8 to 14.4 m B_2= 34.4 to 17.2 m (N=2 to 4) Bin size= <u>30 m</u> (chosen as an appropriate value) RI= <u>60 m</u> SI= <u>60 m</u>

Desired X_{min}*: 500 m	RLI= 240 m (from old surveys in the area) SLI= 360 m (from old surveys in the area) Xmin= $(RLI^2+SLI^2)^{1/2}$ = 432.67 m (less than the shallowest horizon)
Desired X_{max}*: 2700 m	Number of channels in patch= 2000 Number of receiver lines= 20 Channels per line= 100 Cross-line dimension= 4560 m In-line dimension= 6000 Aspect ratio= Cross-line dimension of the patch/ in-line dimension of the patch= 0.76 X_{max}= ½ x [(In-line dimension of the patch)^2 + (Cross-line dimension of the patch)^2]$^{1/2}$ = 3768 m (Should be approx the same as the target depth)
Fold	In-line fold= # rec x RI / (2xSLI)= 100*60/(2*360) = 8.33 Cross-line fold= ½ # Rec. Lines= 13 Total fold= 108.33 (more than the desired but it will introduce fold striping as it is a decimal value)
Migration Apron	Radius of Fresnel Zone= ½ x V_{ave} x (target TWT /f_{dom})$^{1/2}$= ½ (2*2700/2.9)*(2.9/50)$^{1/2}$ = 224.2 m Diffraction energy= 0.58*target depth= 0.58*2700= 1566 m Migration apron= target depth x tan (dip)= 2700*tan(10)= 476 m In-line fold taper= [(in-line fold/2) – 0.5] x SLI= 1320 m Cross-line fold taper= [(cross-line fold/2)-0.5] x RLI= 1440 m (FT+FZ) < total mig apron < (FT+MA) 1320 + 224.2 < TMA < 1440 + 476 = 1544.2 < TMA < 1916 TMA= 1544 m to 1916 m

* Xmin is the largest min offset in a survey and Xmax is the maximum recorded offset. It is usually the half-diagonal distance of the patch

The calculations shown above confirm the validity of parameters chosen for the survey design (table 5).

Table 5. Design Parameters

Source line interval	360 m
Receiver line interval	240 m
Source Station interval	60 m
Receiver Station interval	60 m
Patch	20 x 100

Figure 21 shows the area of study with the source and receiver layout according to orthogonal (left) and slant geometries (right). Source lines are east-west direction and receiver lines are north-south for the orthogonal geometry, and for the slant geometry the receiver lines were changed to 45 degrees. Inside the lakes drawn in these figures, different source and receiver station intervals were tested as the survey is planned to be acquired in winter when the lakes are frozen. Receivers are located every 180 m and sources every 20 m (fewer receivers, more sources). Additionally, some source lines were moved to existing cut lines from previous seismic acquisition in the area, to avoid new line cutting. This is economically and environmentally positive.

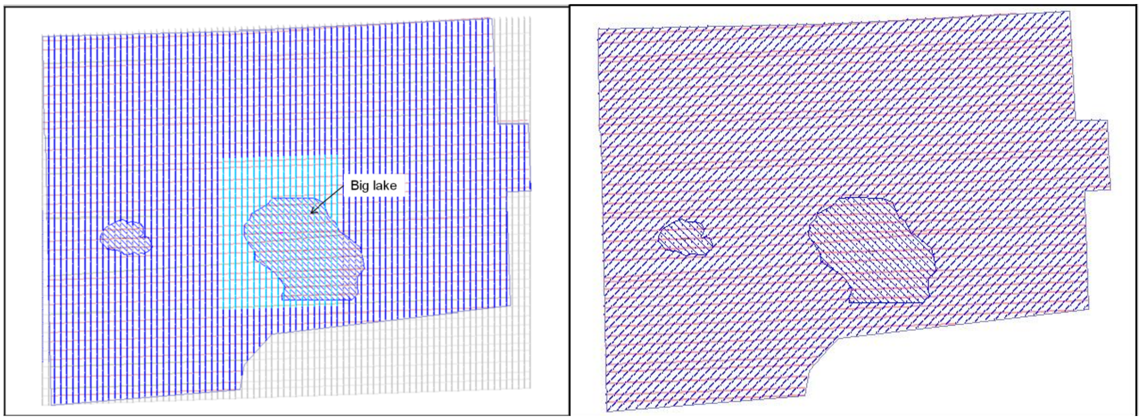

FIG 21. Surface layout, orthogonal (left) and slant (right)

Figure 22 shows the fold for PP survey, with orthogonal geometry (left) and slant geometry (right). Geometry footprint can be appreciated in these figures: we can guess the actual direction of the receiver lines in the slant layout, i.e. 45 degrees, especially around the lake; both of them show the layout of sources (east-west) because some segments of these lines were moved to old cut lines so the source line interval is uneven, producing stripes of low and high fold in the source line direction. The receiver line direction in the orthogonal geometry is not evident; this is the characteristic that is desirable for the entire layout. Also in these figures, ray paths are shown to highlight the influence of the slant layout of receivers over the offset distribution.

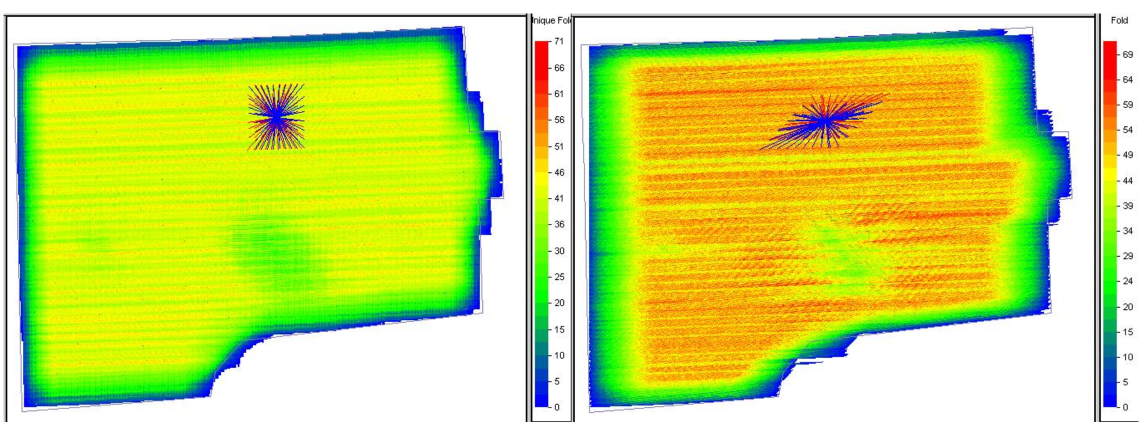

FIG 22. PP survey design fold. Orthogonal (left) and slant (right)

Figure 23 shows the fold for PS survey, with orthogonal geometry (left) and slant geometry (right). The footprint of the surface layout is stronger for orthogonal geometry. Regarding the lake footprint, there is a transition zone from the lowest values inside the lake to the highest values of fold outside the lake for the slant geometry. For the orthogonal geometry this change from lower to higher fold is more abrupt. The area of low fold is smaller for the slant geometry design in both cases (PP and PS).

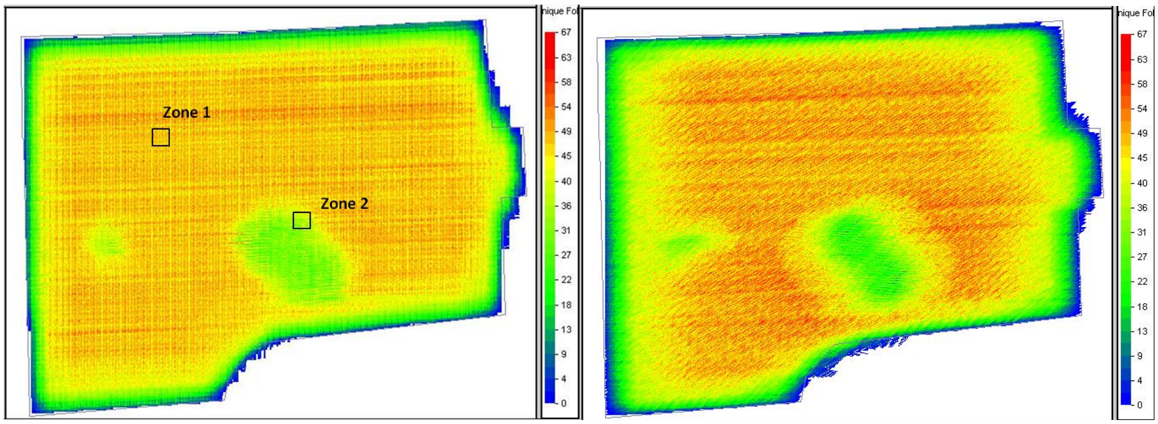

FIG 23. PS Survey design fold. Orthogonal Geom. (left) and slant Geom. (right). Black rectangles show areas of detailed analysis

Seismic attributes for two different areas marked in figure 23 were looked on detail: Zone 1 is an area with no influence of the lakes and zone 2 is an area just in the north east border of the big lake (figures 24-31).

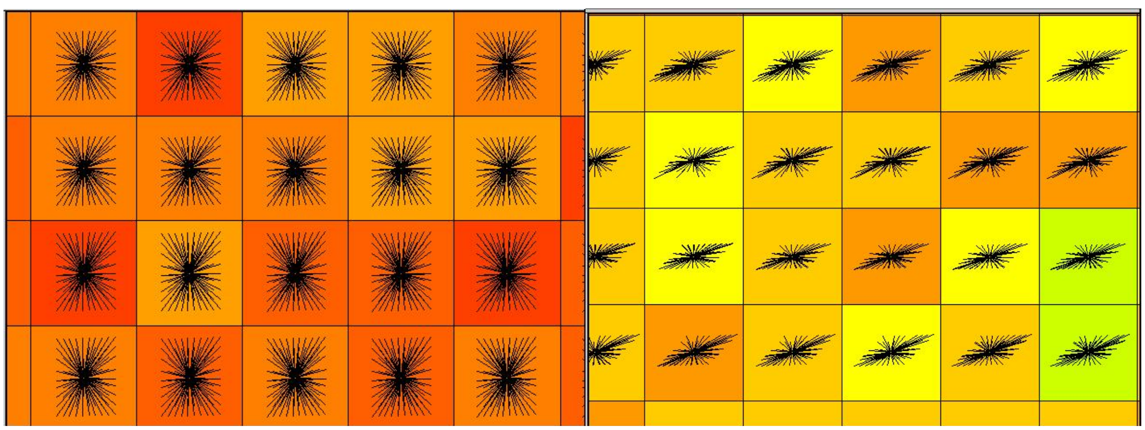

FIG 24. Zone 1: Azimuth – PP survey design – Orthogonal Geom. (left), Slant Geom. (right)

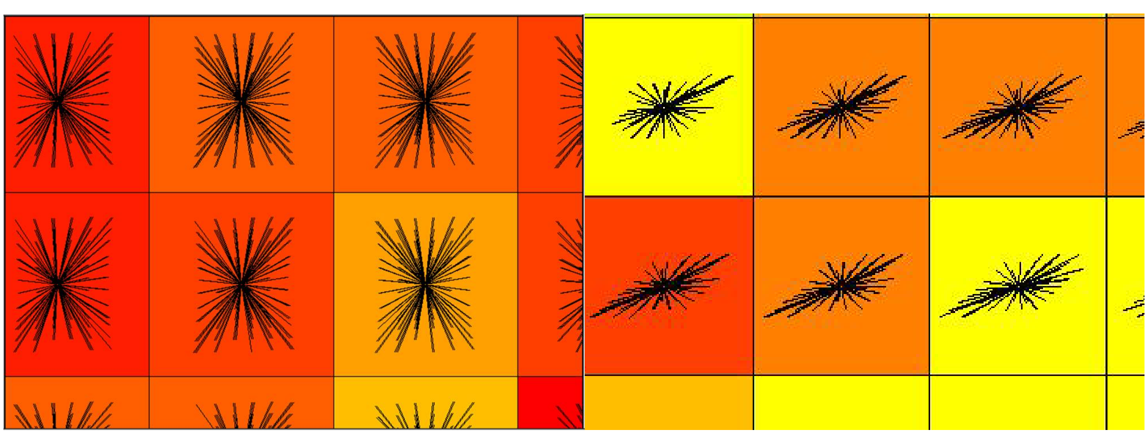

FIG 25. Zone 1: Azimuth – PS survey design – Orthogonal Geom. (left), Slant Geom. (right)

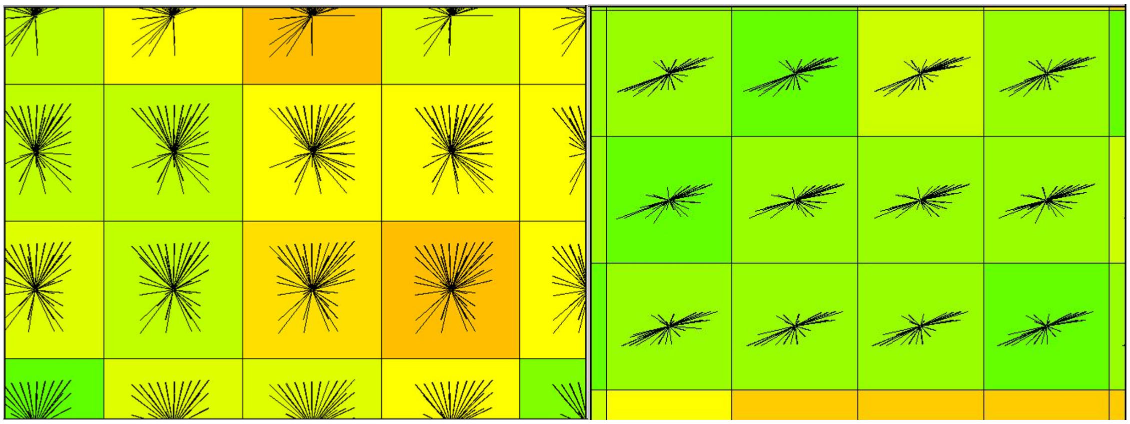

FIG 26. Zone 2: Azimuth – PP survey – Orthogonal Geom. (left), Slant Geom. (right)

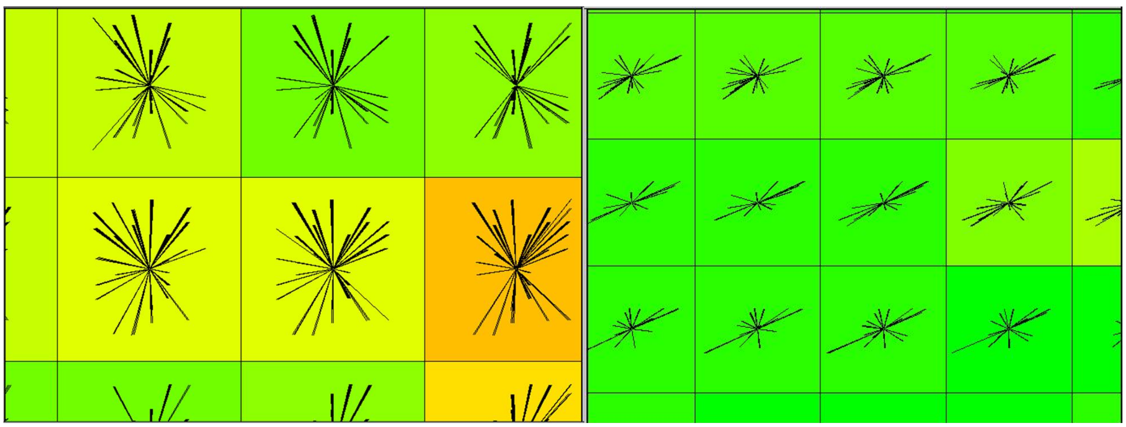

FIG 27. Zone 2: Azimuth – PS survey – Orthogonal Geom. (left), Slant Geom. (right)

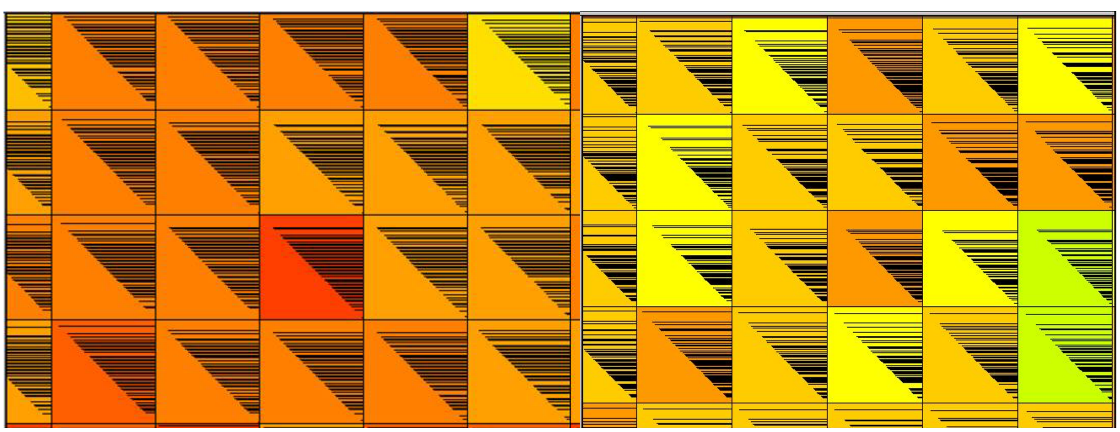

FIG 28. Zone 1: Offset distribution – PP survey – Orthogonal Geom. (left), Slant Geom. (right)

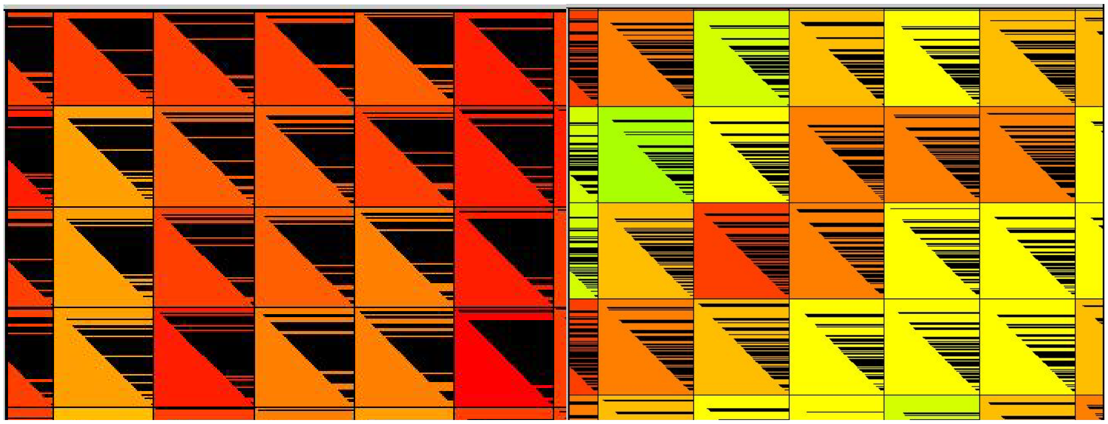

FIG 29. Zone 1: Offset distribution – PS survey – Orthogonal Geom. (left), Slant Geom. (right)

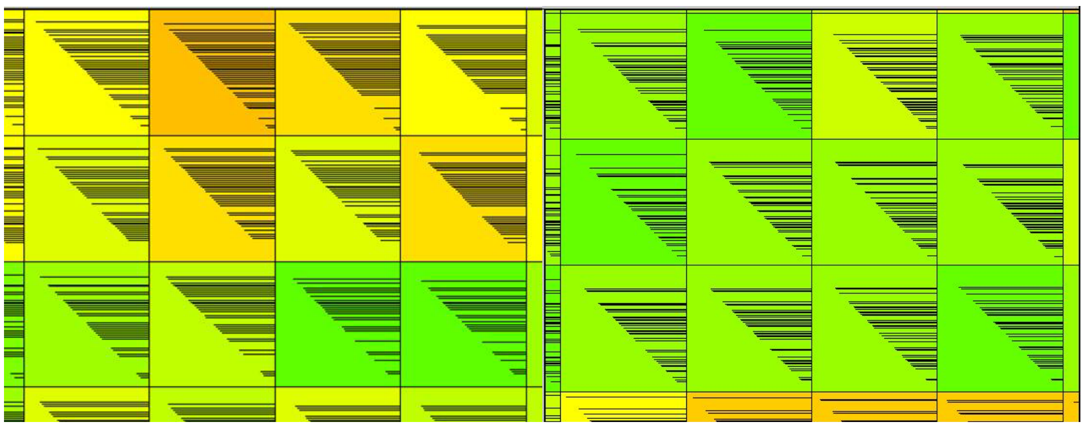

FIG 30. Zone 2: Offset distribution – PP survey – Orthogonal Geom. (left), Slant Geom. (right)

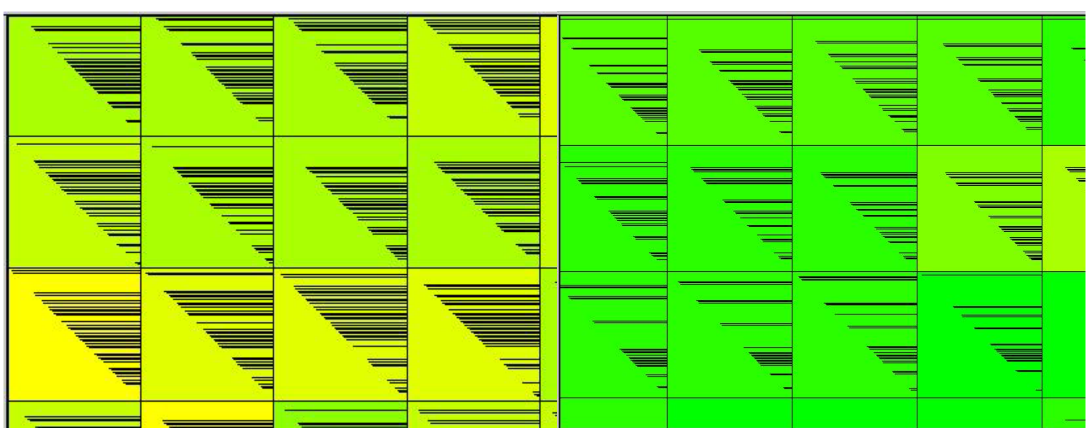

FIG 31. Zone 2: Offset distribution – PS survey – Orthogonal Geom. (left), Slant Geom. (right)

From Figures 24-31, it is concluded that orthogonal geometry produces a better azimuth and offset distribution for data inversion. Offsets and azimuths are lost due to the lake despite increasing the number of shots because the receiver interval was increased. The lost is more obvious for converted waves because there are fewer receivers inside the lake and as it is known, the conversion points are closer to the receivers.

In this case study the slant geometry was produced by laying out receiver lines at 45 degrees, source lines must be in east-west direction to use old cut lines as mentioned earlier. This geometry produced longer offset in the direction of the receiver lines (ray paths in Figure 22). Orthogonal geometry produced a better offset distribution for all azimuths, for this reason it was chosen for the planned seismic acquisition. The stronger footprint produced by the orthogonal geometry on the PS survey can be improved by optimizing design parameters.

For all these experiments, the patch used was 20 lines with 100 receivers per line; this one was changed to 26 lines so that an aspect ratio of 1.0 would be obtained. The reason for this change is to acquire more appropriate data for inversion as mentioned previously.

CONCLUSIONS

- PS surveys can be designed in such a way that can give as good attribute results similar to PP surveys and this will let us take advantage of the new application of the PS surveys such as structural imaging, lithologic estimation, anisotropy analysis, subsurface fluid description and reservoir monitoring.

- Decreasing source line interval improves the seismic attributes (coverage, offset and azimuth).

- Decreasing receiver line interval improves the horizontal discontinuities of coverage.

- The design is improved when considering slant geometry for the shallow target design.

- In the shallow target design, decreasing source line interval increased the number of shots with the consequent increase in survey costs. To balance the quality requirements with cost, a design of source and receiver line interval of 40 m was proposed, which shows good attributes and it would be less expensive than considering 25 m source line interval. The number of receivers increased and the number of shots decreased with this proposal, which is a good characteristic, considering that in land 3C-3D surveys the total source effort is typically about a factor of 2 or 3 times the total receiver effort.

- For the deep target design, orthogonal geometry was chosen because it produced better seismic attribute distributions than the slant geometry. Stripes in the east-west direction can be seen but they are not necessarily product of the design but of the requirement of moving source lines to old cut lines due to environmental concerns. This movement produced stripes of low and high fold that cannot be avoided. The acquisition geometry footprint produced by the orthogonal geometry can be improved by optimizing design parameters, especially the receiver line interval.

- Choosing a geometry that minimizes the possibilities of geometry footprint, improves the quality of stratigraphic mapping, attribute analysis and inversion results.

ACKNOWLEDGMENTS

We would like to thank all CREWES sponsors for their support, the faculty staff and computer technicians in the CREWES project for all their help, Gedco for access to OMNI and Nexen for allowing us to show the deep target design.

REFERENCES

A. Cordsen, M. Galbraith, J. Peirce, 2000, Planning Land 3-D Seismic Surveys, Society of Exploration Geophysicists, Tulsa, p. 201

D. C. Lawton, 1994, Acquisition design for 3-D converted waves, CREWES Research Report Volume 6, 1-23

D. C. Lawton, 1993, Optimum bin size for converted-wave 3-D asymptotic mapping, CREWES Research Report Volume 5, 1-14

D. C. Lawton and B. H. Hoffe, 2000, Some binning issues for 4C-3D OBC survey design, Consortium for Research in Elastic Wave Exploration Seismology (CREWES), University of Calgary, SEG Expanded abstracts

Grace Y.C. Yang, Don C. Lawton, Robert R. Stewart, Susan L. M. Miller, Collin C. Potter, and Vladan Simin, 1996, Interpretation and analysis of the Blackfoot 3C-3D seismic survey, CREWES Research Report Volume 8, 1-46

R. R Stewart., J. E. Gaiser, R. J. Brown, and D. Lawton, 2003, Converted-wave seismic exploration: Applications: Geophysics, 68, 40-57

S. E. Grasby, Z. Chen, A. P. Hamblin, P. R.J. Wozniak, and A. R. Sweet, 2008, Regional characterization of the Paskapoo bedrock aquifer system, southern Alberta: Can. J. Earth Sci., 45, 1501-1516